

Exact microcanonical statistical analysis of transition behavior in Ising chains and strips

K Sitarachu¹, R K P Zia^{2,3,4}, and M Bachmann¹

¹ Soft Matter Systems Research Group, Center for Simulational Physics, Department of Physics and Astronomy, University of Georgia, Athens, GA 30602, USA

² Center for Soft Matter and Biological Physics, Department of Physics, Virginia Tech, Blacksburg, VA 24061, USA

³ Department of Physics & Astronomy, University of North Carolina at Asheville, Asheville, NC 28804, USA

⁴ Physics Department, University of Houston, Houston, Texas 77204, USA

Abstract. Recent analyses of least-sensitive inflection points in derivatives of the microcanonical entropy for the two-dimensional Ising model revealed higher-order transition signals in addition to the well-studied second-order ferromagnetic/paramagnetic phase transition. In this paper, we re-analyze the exact density of states for the one-dimensional Ising chain as well as the strips with widths/lengths of up to 64/1024 spins, in search of potential transition features. While some transitions begin to emerge as the strip width increases, none are found for the chain, as might be expected.

Submitted to: *J. Stat. Mech.*

1. Introduction

The (Lenz-)Ising model [1, 2] is one of the simplest spin models for the study of ferromagnetic order in crystals. Conventional statistical analysis of the exactly solvable one-dimensional (1D) model [2] did not reveal thermodynamic phase transition features at finite temperatures, though, despite significant energy fluctuations. However, the two-dimensional (2D) problem, which was first solved exactly by Onsager by means of canonical statistical analysis [3], exhibits common signatures of a second-order phase transition between the disordered paramagnetic and the ordered ferromagnetic phase. The simplicity of the model made it a popular standard model for investigating complexity and triggered a vast number of theoretical studies aimed at a more general understanding of thermodynamic phase transitions. It also significantly contributed to the development of computational statistical physics as advanced algorithmic methodologies such as Monte Carlo sampling and finite-size scaling strategies enabled a better understanding of how short-range interaction can cause long-range order under thermal conditions.

The canonical statistical analysis method used in most of these studies works particularly well for very large systems, where the assumption of negligible surface contact of the system of interest with the surrounding heat bath is justified and the heat bath temperature can be considered a suitable and adjustable parameter controlling the equilibrium properties of the system. One of the important consequences is that different response quantities and an appropriate order parameter indicate the catastrophic fluctuations accompanying a phase transition at a unique transition point. For finite systems, this is not the case and the identification of a transition *point* is not generally possible; different response quantities suggest different transition points. It is therefore common to extrapolate data obtained in computer simulations, where only systems of finite size can be simulated, toward the thermodynamic limit by finite-size scaling. This is particularly useful for the analysis of second-order transitions where the system loses its identity close to the phase transition point in the thermodynamic limit. All fluctuating quantities are non-analytic at the same transition point and can be quantified by power laws with specific critical exponents.

However, the recent enormous advances in the development of technologies that makes possible experiments and applications on nanoscales has increased the interest of interdisciplinary sciences like biochemistry in using statistical physics methods for the understanding of complex behavior and long-range cooperativity in *finite systems*. Thus, the foundation of the statistical methods that have been so successful in understanding phase transitions in large systems needs to be extended to include systems such as proteins for which the thermodynamic limit is an inappropriate assumption [4].

The recently introduced generalized microcanonical inflection-point method [5] was developed to overcome these issues. It ultimately enables the systematic identification and even classification of transition signals in systems of arbitrary size.

In this paper, we revisit the one-dimensional (1D) Ising spin chain and extend our

study to Ising strips with $L \times M$ spins attached to the nodes of a square lattice with L being the length and M the finite width of the strips. It has long been known that the 1D Ising chain does not experience a thermodynamic phase transition at finite temperatures [2]. However, the specific heat curve exhibits interesting monotonic features. It is important to note that such features like peaks in quantities such as the specific heat are indeed often used as signals of cooperative behavior in systems of finite size, in particular those that do not possess a thermodynamic limit (e.g., finitely long, heterogeneous systems such as proteins). Since the thermodynamic limit represents an artificial situation, canonical statistical analysis faces the dilemma of not being able to rigorously distinguish transitions signatures in finite systems that might correspond to phase transitions in the thermodynamic limit from those that do not. For this reason, it is instructive to consider the exact, microcanonical solution of the 1D Ising chain first. We then study the properties of the more interesting 2D systems, i.e., the periodic Ising strips of length L and width M , using the exact analytic method of Beale [6], which is based on Kaufman’s solution of the Ising model [7]. We consider both narrow ($M = 3, 4$) and broader strips ($M = 32, 64$). Both types of strips display novel transitions absent for the chain ($M = 1$), though the ones for the broader strips appear to be closer in nature to those found recently [5, 8] for the Ising system on a square lattice (L^2). We have no reason to doubt that these additional transition features of higher order would not survive in the thermodynamic limit.

2. Ising chain and Ising strips

In the Ising systems we study, the energy of a spin configuration $\mathcal{S} = (s_1, s_2, \dots, s_N)$, with $s_i = \pm 1$, on a rectangular lattice with L spins in one direction and M spins in another ($N = LM$) can be written as

$$E(\mathcal{S}) = -J \sum_{\langle i,j \rangle} s_i s_j, \quad (1)$$

where $\langle i, j \rangle$ indicates that only interactions of nearest-neighbor spin pairs s_i and s_j are considered. For $J > 0$, ferromagnetic coupling energetically favors spins in the same state, whereas for antiferromagnetic coupling ($J < 0$), configurations of alternating spins are energetically preferred. For the discussion of the microcanonical results it is already useful to note that for odd choices of L and/or M the total numbers of states with negative and positive energies, respectively, are not identical. Thus, the athermal energy distribution $g(E)$ (“density” of states[‡]) cannot be symmetric.

In this study, we re-visit the one-dimensional Ising chain with L spins ($M = 1$) and periodic boundary conditions (rings). For the two-dimensional Ising strips, we investigate the cases $M = 3$ and $M = 4$, respectively, with periodic boundary conditions

[‡] In fact, since the problem is discrete, one should call this quantity the “number of states,” but density of states is a more commonly used term even in this context.

in both directions (tori).[§] Eventually, this analysis is extended to broader strips with $M = 32$ and $M = 64$.

The exact solutions for the quantities needed for the statistical analysis are known, at least in principle. Revisiting the 1D case is useful for comparison. For the 2D Ising systems, the calculation of microcanonical quantities like the density of states requires algorithmic procedures [6] and for large systems it is common to use stochastic methods like Monte Carlo sampling to obtain estimates for the density of states [9]. Here, we consider only finite systems and all analyses are exact. In the following, we first investigate the 1D Ising case from the perspective of microcanonical statistical analysis in search of transition signals and then study transition features of the 2D strips.

3. Canonical Statistical Analysis of the One-Dimensional Ising Chain

For $M = 1$, the energy function of the Ising model (1) represents the 1D Ising chain with L spins:

$$E(\mathcal{S}) = -J \sum_{l=1}^L s_l s_{l+1}, \quad (2)$$

where $s_{L+1} = s_1$ to satisfy periodic boundary conditions. The canonical partition function, which is the basis for the conventional canonical statistical analysis, is given by

$$Z = \sum_{\{\mathcal{S}\}} e^{-\beta_{\text{th}} E(\mathcal{S})} \quad (3)$$

where $\beta_{\text{th}} = 1/k_{\text{B}}T$ is the inverse thermal energy. The sum is over the complete space of spin configurations. Using the eigenvalues of the transfer matrix

$$\lambda_+ = 2 \cosh(\beta_{\text{th}} J), \quad \lambda_- = 2 \sinh(\beta_{\text{th}} J) \quad (4)$$

the solution can be written as

$$Z = \lambda_+^L + \lambda_-^L. \quad (5)$$

Since $\lambda_+ > \lambda_-$, the contributions of λ_- to thermodynamic quantities vanish in the thermodynamic limit $L \rightarrow \infty$. This approximation is typically used to show that there cannot be a phase transition in the 1D case [10]. However, for our following discussion, which includes finite-size properties, it is necessary to keep working with the full solution. The internal energy of the system is given by

$$\langle E \rangle = -\frac{\partial}{\partial \beta_{\text{th}}} \ln Z. \quad (6)$$

From it, a somewhat lengthy expression for the specific heat (heat capacity per spin)

$$c = \frac{1}{L} \frac{\partial \langle E \rangle}{\partial T}. \quad (7)$$

[§] We do not consider $M = 2$, because periodic boundary conditions are somewhat ambiguous in this case.

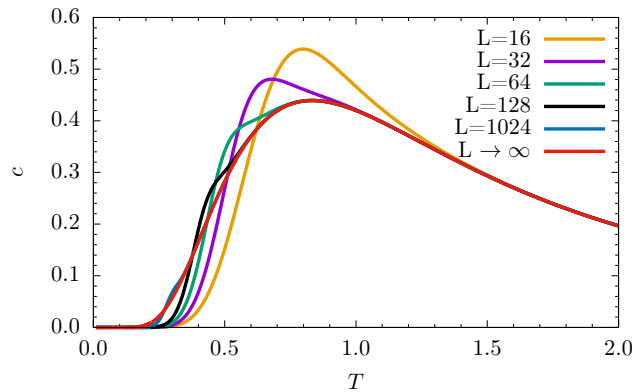


Figure 1. Exact specific heat curves $c(T)$ for the one-dimensional Ising chain for various chain lengths L .

can easily be obtained after some algebra. In the thermodynamic limit,

$$\lim_{L \rightarrow \infty} c = k_B \beta_{\text{th}}^2 J^2 \text{sech}^2(\beta_{\text{th}} J). \quad (8)$$

Curves of $c(T)$ are shown in Fig. 1 for various finite chain lengths L and in the thermodynamic limit $L \rightarrow \infty$. Already for $L = 1024$, the curve is virtually indistinguishable from the well-known result in the thermodynamic limit.

One interesting aspect is the way the peak for $L = 16$ disappears, because it does not actually seem to converge to the peak location apparent for $L \rightarrow \infty$. Rather, with increasing chain length, it drifts to lower temperatures and the peak height decreases. For $L = 64$, only a prominent “shoulder” remains (and the peak at about $T = 0.8$, which survives for $L \rightarrow \infty$, has formed). Increasing L further, the “shoulder” becomes weaker and keeps shifting toward lower temperatures. For $L \rightarrow \infty$ it is completely gone. The height of the remaining peak is finite in this limit. As expected, the 1D Ising chain does not experience a thermodynamic phase transition. Thus, as a general conclusion, a peak in a specific-heat curve does *not necessarily* signal a significant qualitative change of the thermodynamic macrostate of the system at the temperature associated with the specific heat peak.

Now the problem of this argumentation is, however, that for systems, which are necessarily of finite size (like biologically relevant macromolecules or nanoscale devices), peaks or “shoulders” in specific heat curves and other response quantities are the only available signals and often indeed considered important indicators of structural transitions in such systems. In heterogeneous systems like proteins, finite-size scaling analysis is not applicable and thus it is not possible to test if a non-analyticity might develop in the hypothetical thermodynamic limit. On the other hand, the typically highly cooperative qualitative changes in these systems can be substantial, and it is more than just tempting to consider these processes analogs of phase transitions in finite systems^{||}. In consequence, conventional canonical statistical analysis cannot resolve this

^{||} It has been common to call representative ensembles of macrostates in finite systems “pseudophases”

dilemma. The recently developed generalized microcanonical inflection-point analysis method [5] was introduced to offer an alternative, consistent, and more systematic approach to identify and even classify transitions in systems of any size. After a brief introduction, we apply it to the 1D Ising chain, which will allow us to decide whether or not the peaks and shoulders in the specific heat curves in Fig. 1 might indicate a hidden transition that simply does not develop into a phase transition or whether these canonical features are indeed irrelevant in the context of macroscopic cooperative behavior.

4. Generalized microcanonical inflection point analysis

The microcanonical entropy version of Boltzmann’s formula,

$$S(E) = k_B \ln g(E), \quad (9)$$

has long been used as an alternative basis for identifying first-order transition signals, which, for finite systems, show a distinctive “convex intruder” in the otherwise strictly concave monotonic behavior of this quantity. In the thermodynamic limit, the convex region disappears and becomes linear [11]. Considering inflection points in the first derivative of $S(E)$, i.e., in the microcanonical inverse temperature

$$\beta(E) = \frac{dS(E)}{dE}, \quad (10)$$

as indicators enabled the extension to second-order transitions [12]. The recently introduced generalized microcanonical inflection-point analysis method makes use of the principle of least sensitivity [13, 14]. Least-sensitive inflection points in all derivatives of $S(E)$ are analyzed systematically to identify and classify transitions of any order [5], similar to Ehrenfest’s classification approach, which is based on thermodynamic potentials [15]. However, the great advantage of the novel microcanonical method is that it can be employed for systems of any size and does not hinge on the thermodynamic limit.

In fact, the consequent application of the method leads to the introduction of two types of transitions: *Independent* transitions, which are not associated with any other transition signals, and *dependent* transitions that can only coexist with a corresponding independent transition. A dependent transition, if it exists, can only occur at a higher energy (or temperature) and has always a higher order than the independent transition it is associated with. Consequently, there’s no first-order dependent transition. These dependent transitions can be considered valuable precursor signals in the disordered phase of imminent ordering upon lowering system energy (or temperature).

Formally, a phase transition is defined in the generalized microcanonical inflection-point analysis method by a corresponding least-sensitive inflection point in $S(E)$ or any of its derivatives at the transition energy E_{tr} . For practical purposes, it is useful to and the crossovers between these “pseudophase transitions,” but this is a rather unsatisfying way of dealing with this problem.

identify the extremal point in the next-higher derivative. Consequently, for *independent transitions* of odd order $(2k-1)$ (k positive integer), the valley of the $(2k-1)$ th derivative has a positive-valued minimum at the transition energy E_{tr} ,

$$\left. \frac{d^{(2k-1)}S(E)}{dE^{(2k-1)}} \right|_{E=E_{\text{tr}}} > 0, \quad (11)$$

and for even order $2k$ the peak of the $(2k)$ th derivative at E_{tr} is negative-valued:

$$\left. \frac{d^{2k}S(E)}{dE^{2k}} \right|_{E=E_{\text{tr}}} < 0. \quad (12)$$

The lowest-possible order of a *dependent transition* is 2. In general, dependent transitions of even order $2k$ are characterized by

$$\left. \frac{d^{2k}S(E)}{dE^{2k}} \right|_{E=E_{\text{tr}}^{\text{dep}}} > 0, \quad (13)$$

whereas for odd order $(2k+1)$:

$$\left. \frac{d^{(2k+1)}S(E)}{dE^{(2k+1)}} \right|_{E=E_{\text{tr}}^{\text{dep}}} < 0. \quad (14)$$

must be satisfied. For brevity, we introduce in addition to $\beta(E)$ given in Eq. (10) the following symbols for higher-order derivatives: $\gamma(E) = d^2S(E)/dE^2$, $\delta(E) = d^3S(E)/dE^3$, $\epsilon(E) = d^4S(E)/dE^4$, etc.

Remarkably, for the 2D Ising model with L^2 spins, not only the expected ferromagnetic-paramagnetic transition was recovered and correctly classified as a second-order transition with this method. Two additional transitions, a dependent transition above and an independent transition below the critical temperature were discovered [5, 8]. For sufficiently large systems, these transitions are of third order and the extrapolation of the exact data calculated for finite systems with up to $N = 192^2$ spins suggests that they would survive in the thermodynamic limit (see Fig. 2).

4.1. Statistical analysis for the 1D Ising chain

The inflection-point analysis for the 1D model is straightforward and all results for any spin chain length are easily found analytically. For simplicity, we consider an even number of spins L and periodic boundary conditions. It is convenient to introduce the number b of “broken” bonds. A single broken bond represents an energy increase by $2J$. Now, a spin flip affects a pair of bonds and only if both are broken after the flip, the energy increases. Thus, b must be an even integer. The total energy of a spin configuration is then given by

$$E_b = (-L + 2b)J, \quad b = 0, 2, 4, \dots, L. \quad (15)$$

Simple combinatorics yields the number of configurations g_b for b broken bonds. We exploit the route of the canonical partition function (3), since it can be expressed as a sum over the number of states g_E with given energy E :

$$Z = \sum_E g_E e^{-\beta_{\text{th}}E} = \sum_b g_b e^{-\beta_{\text{th}}E_b}. \quad (16)$$

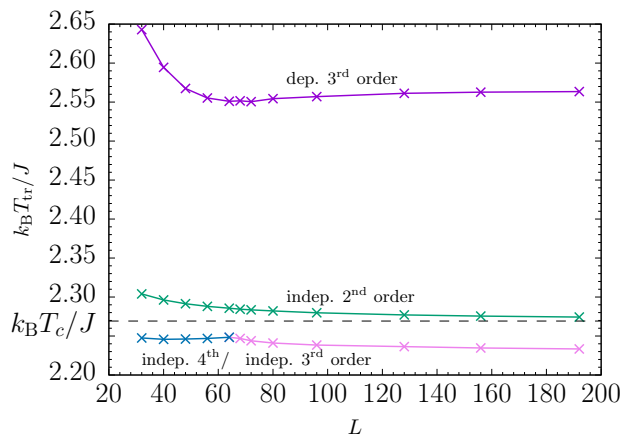


Figure 2. The recent microcanonical inflection-point analysis for the full 2D Ising model [5, 8] correctly identified the second-order transition, which becomes critical at $k_B T_c / J = 2 / \ln(1 + \sqrt{2})$ in the thermodynamic limit, but two additional higher-order signals were found as well (lines are guides to the eye).

Making use of the solution (4) and the binomial expansion yields

$$Z = 2 \sum_{b=0,2,4,\dots}^L \binom{L}{b} e^{-\beta_{\text{th}} E_b} \quad (17)$$

and thus

$$g_b = 2 \binom{L}{b}, \quad (18)$$

as expected. With this, we can define the microcanonical entropy

$$S_b = k_B \ln g_b. \quad (19)$$

Curves of S_b are shown in Fig. 3(a) for several chain lengths.

As analogs of the continuous derivatives, we employ the following discrete, symmetric differences:

$$\beta_{E_b} = \frac{S_{b+2} - S_{b-2}}{2\Delta E_b}, \quad (20)$$

$$\gamma_{E_b} = \frac{S_{b+2} - 2S_b + S_{b-2}}{(\Delta E_b)^2}, \quad (21)$$

$$\delta_{E_b} = \frac{S_{b+4} - 2S_{b+2} - 2S_{b-2} - S_{b-4}}{2(\Delta E_b)^3}, \quad (22)$$

$$(23)$$

where $\Delta E_b = 4J$. For the subsequent analysis, we set the irrelevant constants to unity, $J \equiv 1$ and $k_B \equiv 1$.

If there was a first-order transition, S_b should have a least-sensitive inflection point indicated by a positive-valued minimum in

$$\beta_{E_b} = \frac{1}{8} \ln \frac{(L-b+2)(L-b+1)(L-b)(L-b-1)}{(b+2)(b+1)b(b-1)}, \quad (24)$$

which obviously does not exist for the 1D Ising chain. Introducing the parameter $x_b = b/L$, Taylor expansion yields for $0 < x_b < 1$ (i.e., explicitly excluding the edges $x_b = 0$ and $x_b = 1$)

$$\beta_{E_b} = \frac{1}{2} \ln \frac{1-x_b}{x_b} + \frac{1}{4} \frac{2x_b-1}{x_b(1-x_b)} \frac{1}{L} + \mathcal{O}(1/L^2). \quad (25)$$

Thus, in the thermodynamic limit $L \rightarrow \infty$, β_{E_b} converges to $(1/2) \ln[(1-x_b)/x_b]$ for any given value $x_b \in (0, 1)$. Figure 3(b) shows the β_{E_b} curves for various chain lengths L . The quick convergence of the curves to the result in the thermodynamic limit is already apparent for small chain lengths. In the typically only considered negative-energy region, associated with positive temperatures, β_{E_b} does not exhibit inflection points at any chain length. The same applies in the generally ignored positive-energy (negative-temperature) space. However, since β_{E_b} is convex for $E_b < 0$ and concave for $E_b > 0$, it possesses a least-sensitive inflection point at $E_b = 0$. This is confirmed by the associated peak in

$$\gamma_{E_b} = \frac{1}{16} \ln \frac{(L-b)(L-b-1)b(b-1)}{(L-b+2)(L-b+1)(b+2)(b+1)} \quad (26)$$

$$= -\frac{1}{4} \frac{1}{x_b(1-x_b)} \frac{1}{L} + \mathcal{O}(1/L^2). \quad (27)$$

According to our classification scheme, this signals an independent, but thermodynamically irrelevant, second-order transition in the 1D model at $\beta = 0$ that does not disappear in the thermodynamic limit. Note that, despite formally being of second order in our scheme, this is not a critical transition; the appropriately scaled derivative $\gamma \times L$ does not vanish in the thermodynamic limit [see Fig. 3(c)]. Although this example is not particularly interesting, it shows that discontinuous, critical transitions represent only a subset of second-order transitions in this scheme.

Eventually, we find

$$\delta_{E_b} = \frac{1}{128} \ln \frac{(L-b+4)(L-b+3)(L-b-2)(L-b-3)}{(L-b+2)(L-b+1)(L-b)(L-b-1)} \times \frac{(b+2)(b+1)b(b-1)}{(b+4)(b+3)(b-2)(b-3)}, \quad (28)$$

$$= -\frac{1}{8} \frac{2x_b-1}{x_b^2(1-x_b)^2} \frac{1}{L^2} + \mathcal{O}(1/L^3) \quad \forall x_b \in (0, 1) \quad (29)$$

and, as shown in Fig. 3(d), the scaled $\delta \times L^2$ curves do not reveal any features of higher-order transitions.

To conclude, microcanonical inflection-point analysis does not uncover any transition features among the equilibrium states of the 1D Ising model. This confirms the expected result from conventional analysis, although response quantities like the specific heat show pronounced thermal activity, which in fields like the polymer sciences is often considered a sign of significant cooperative behavior. This can lead to confusion or an ambiguity of interpretations for finite systems, which the microcanonical analysis method used here does not allow.

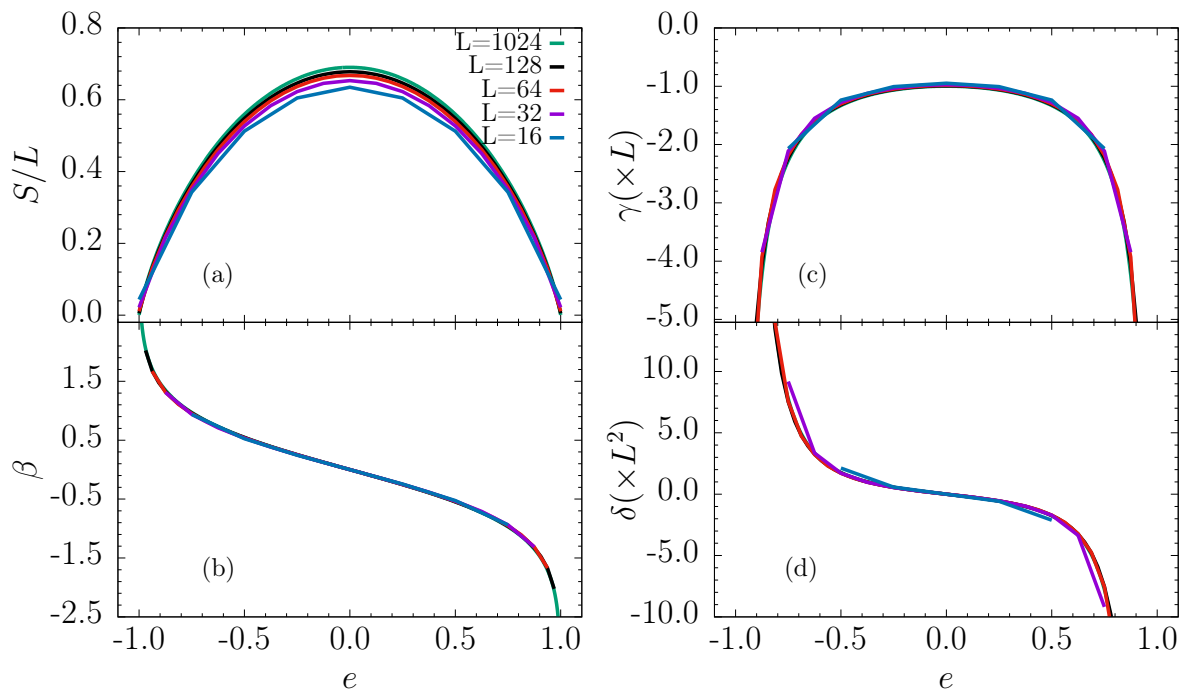


Figure 3. Microcanonical curves of the 1D Ising chain for different chain lengths L as a function of $e = E_b/L$ (lines are guides to the eye.)

4.2. Transition properties of narrow Ising strips

In order to investigate the onset of the paramagnetic-ferromagnetic phase transition in the 2D Ising model, we extend our consideration from the 1D Ising chain (ring) to 2D strips (tori with finite tube diameter). We initially choose to study the $L \times 3$ and $L \times 4$ systems (with L even as before) with periodic boundary conditions in both dimensions. This will allow us to discuss potential differences in the phase behavior for systems that are finite in the second dimension and (non)symmetric under periodic boundary conditions. Later on, we will study the impact of M on the transition signals by investigating broader strips.

Since the focus will be on the microcanonical analysis and interpretation, we use the algorithmic solution by Beale for the exact number of states g_E [6] to calculate the microcanonical entropy and its derivatives needed for our analysis. This method makes use of the low-temperature expansion for the partition function of the $L \times M$ Ising model with periodic boundary conditions, which was first calculated by Kaufman [7].

For comparison, we also use g_E to determine the canonical moments of the energy and from these the specific heat,

$$c = \frac{1}{LMk_B T^2} (\langle E^2 \rangle - \langle E \rangle^2), \quad (30)$$

which is shown in Fig. 4(a) for both $M = 3$ and $M = 4$ and various strip lengths L . Apparently, the curves for each scenario fall almost on top of each other, which, similarly to the 1D case, suggests that c does not exhibit singular scaling properties.

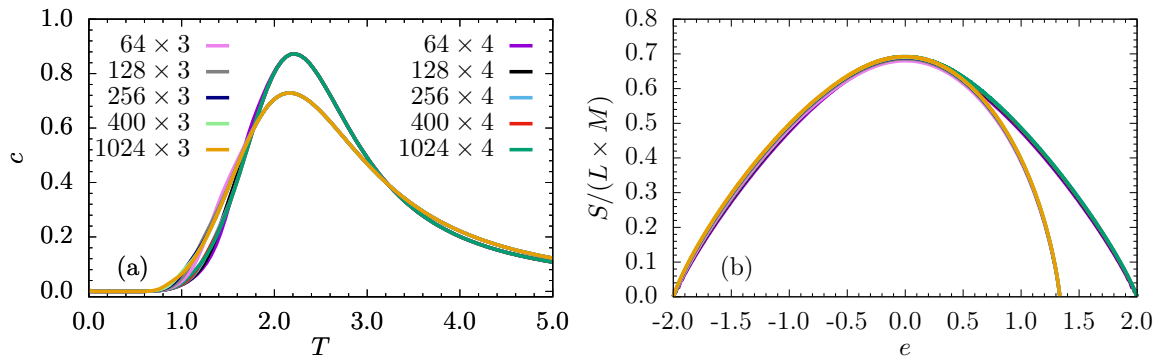


Figure 4. (a) Specific heat curves $c(T)$ and (b) microcanonical entropies $S(e)$ with $e = E/LM$ for $L \times M$ Ising strips with $M = 3, 4$ at various chain lengths L . Note that both figures contain two sets of curves.

Broadening the 1D chain to a narrow strip does not enforce a spontaneous breaking that could cause a phase transition (for a recent review on spontaneous symmetry breaking, see Ref. [10]).

It is noteworthy, though, that the peak value for the broader strip ($M = 4$) is larger than for the smaller one, which indicates the development of a transition signal upon increasing M . We will further elaborate on this in the subsequent discussion of broader strips with $M = 32, 64$. For now it is sufficient to observe that the sole introduction of a second dimension does not lead to a thermodynamic phase transition in the system. Conventional canonical statistical analysis thus discards this scenario as not being thermodynamically interesting. But what does the microcanonical analysis yield?

In Fig. 4(b), the microcanonical entropy curves are shown for both cases. As expected, the curves for $M = 3$ are nonsymmetric, because fewer positive energy configurations are possible (as they favor antiferromagnetic alignments while periodic boundary conditions lead to frustration). Like in the 1D case, the entropies scale with system size LM in the reduced energy space $e = E/LM$. The entropy curves do not show significant features so let us now focus on the derivatives plotted in Figs. 5(a)–(d). In fact, the microcanonical results are very intriguing, although they also do not show any indication of critical behavior in the thermodynamic limit.

Like in the 1D case, the first derivative $\beta(e)$ is virtually scale independent, but in striking contrast to the 1D case, there is no least-sensitive inflection point at $e = 0$ anymore. Instead, in the symmetric case $L \times 4$, it has been replaced by a pair of inflection points *within* $e \neq 0$ regions. These signals of independent second-order transitions, which appear prominently as peaks in the γ curves for $L \times 4$ [Fig. 5(b)], mark the existence of the boundaries between the disordered paramagnetic phase (with e around 0) and the familiar ordered ferromagnetic phase (in the $e < 0$ region), as well as the less familiar antiferromagnetic phase (with $e > 0$, corresponding to negative microcanonical temperatures). This is the precursor to the known behavior of the 2D Ising system in the thermodynamic limit (in both dimensions). Hence we confirm that this qualitative

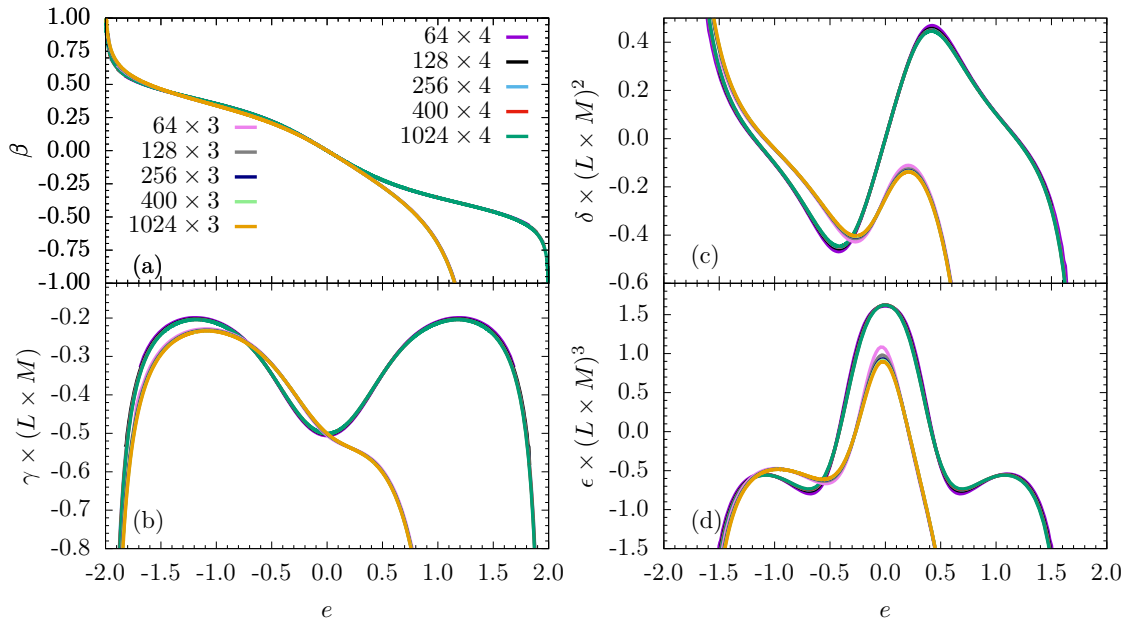


Figure 5. Derivatives of the microcanonical entropies for the $L \times 3$ and $L \times 4$ Ising strips.

change in $\beta(e)$ accompanied by the creation of a new phase is caused by the sole existence of the second dimension.

The nonsymmetric system falls short of developing a second-order transition signal in the positive-energy space due to lack of available microstates, but the least-sensitive inflection point in $\gamma(e)$ at $e \approx 0.2$ suggests a (dependent) third-order transition in addition to the prominent second-order signal in the negative- e region. Though we have not studied systems with odd strip widths $M > 3$, there are good reasons to believe that this asymmetry will fade away as M becomes large. ¶

Both systems possess another independent transition of fourth order (again two symmetric signals for $L \times 4$, but one only for $L \times 3$), as indicated by the least-sensitive inflection points in $\delta(e)$.

Figure 6 summarizes all information about the transition points identified in the canonical and microcanonical analysis of the various systems sizes studied. For the discussion of equilibrium behavior only non-negative temperatures are relevant. The dashed line is located at the critical temperature of the 2D Ising system in the thermodynamic limit and serves as a reference. First of all, as already expected, none of the transition curves shows any trend to converge to the critical point in the thermodynamic limit, but the fact that the signals do not disappear or “fade out” either is remarkable. It tells us that the inherent phase structure of the 2D Ising system is already present in the narrow Ising strip scenarios, although critical behavior is not achieved even for infinitely long strips ($L \rightarrow \infty$). The transition temperatures found for

¶ We should note that, if we had imposed free boundary conditions instead of periodic ones, there would be no asymmetry.

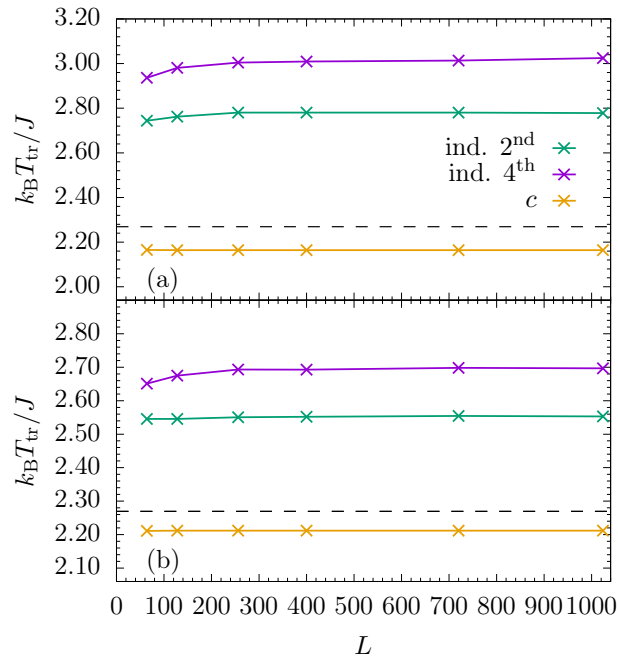


Figure 6. Dependence of the microcanonical transition temperatures on strip length L for strip widths (a) $M = 3$ and (b) $M = 4$. Analyses were done for lengths marked by a cross. For comparison, the peak temperatures of the specific heat c are also included in the figures for the respective strip parameter values. Lines are guides to the eye only. The horizontal dashed lines are located at the critical temperature of the 2D Ising model in the thermodynamic limit, $k_B T_c / J = 2 / \ln(1 + \sqrt{2})$.

$M = 4$ are closer to the critical point of the 2D Ising model than those identified for $M = 3$.

4.3. Qualitative changes for broader Ising strips

The results discussed above provoke the question, whether or not there is a finite threshold strip width M , beyond which the Ising strip develops symptoms of critical behavior. In order to keep the ability of using the Beale method to obtain exact microcanonical results, we restrict our discussion to widths $M = 32$ and $M = 64$. We also investigate only the thermodynamic behavior at positive microcanonical temperatures (i.e., negative energies).

Let us first take a look at the specific-heat curves shown in Fig. 7. For $M = 32$, we observe that initially the peak height increases, but for strip lengths $L > 96$, it decreases again and converges to a finite height, similar to the 1D case. If $M = 64$, the peak of the specific heat is almost independent of L , although we still notice a slight decrease of the peak height upon increasing L for $L > 128$. The peak heights are higher and the peak regions narrower for the broader strip, supporting the development of the expected singularity at the critical temperature in the limits $M \rightarrow \infty$ and $L \rightarrow \infty$. From the 1D case we know that a peak in the specific heat curves does not necessarily mean that the

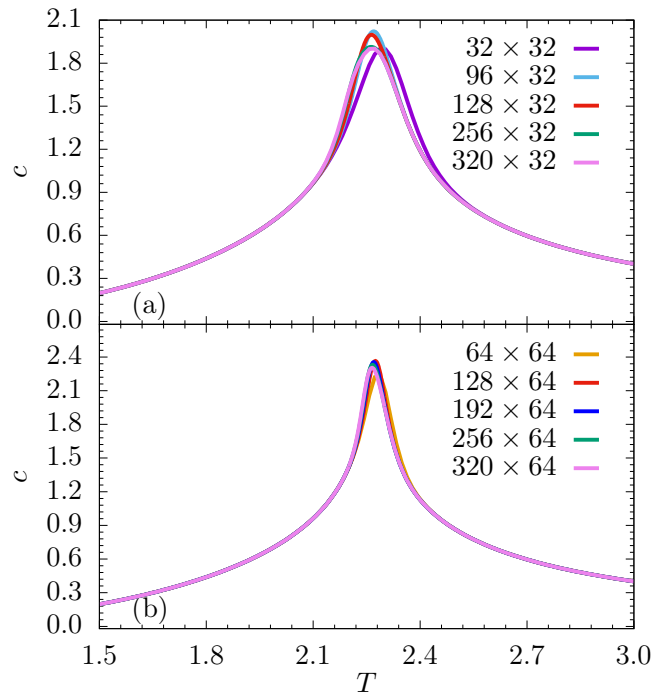


Figure 7. Specific heat curves $c(T)$ for Ising strips with (a) $M = 32$ and (b) $M = 64$ at various chain lengths L .

system undergoes qualitative macrostate changes. However, the microcanonical analysis seems to be more capable of distinguishing significant from insignificant fluctuations. In contrast to the 1D case we found noticeable transition features for the narrow Ising strips as discussed above. This encourages the use of the microcanonical approach for the broader strips, too.

Entropy curves are not shown here, because they do not exhibit any striking monotonic feature of interest. Furthermore, the first derivative [or $\beta(e)$; not shown either] only exhibits a single obvious least-sensitive inflection point indicating a second-order transition for all studied systems sizes with $M = 32$ and $M = 64$. The corresponding peaks are clearly present in the next-higher derivative $\gamma(e)$ shown in Figs. 8(a) and (d). In this context it is important to notice that the peak height drops, which effectively means that the inflection point in $\beta(e)$ becomes *more sensitive the larger the system size*. This leads to the conclusion that whereas the second-order signal is prominent and does not show any tendency of disappearing in the thermodynamic limit, the transition is not “thermodynamic” in the traditional sense. For this to be the case, the peak in $\gamma(e) \times LM$ must converge to zero, which essentially means that the inflection point in $\beta(e)$ becomes a saddle point and thus *minimally sensitive*. The transition signal we observe, however, is remarkable as the peak locations converge toward the 2D Ising transition point in energy space (vertical dashed line in Fig. 8 associated with the critical point in temperature space). Figure 9 shows the microcanonical transition temperatures versus the strip lengths for both $M = 32$ and

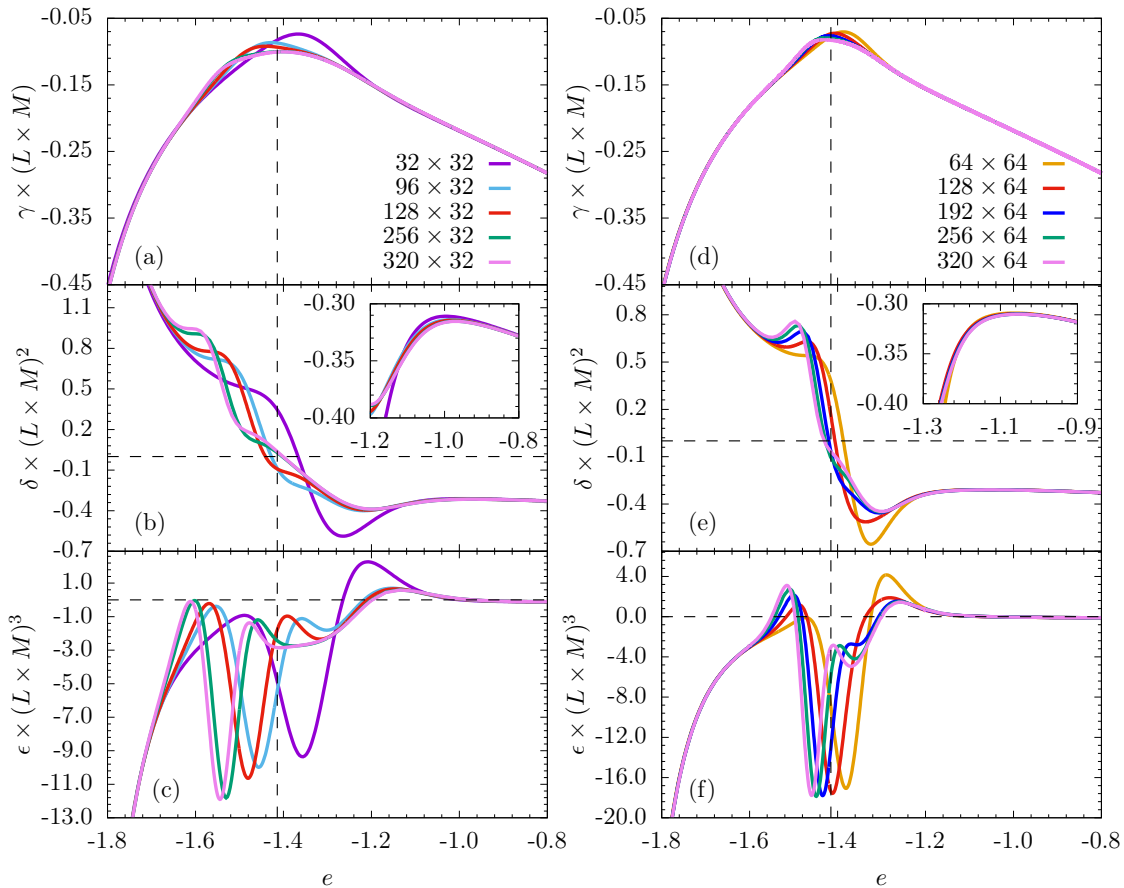


Figure 8. Derivatives of the microcanonical entropies for the $L \times 32$ and $L \times 64$ Ising strips. Horizontal dashed lines mark zero and vertical dashed lines are located at the transition energy associated with the critical transition temperature of the 2D Ising model.

$M = 64$. The second-order signals very quickly converge to the critical temperature (dashed line) for larger systems. Thus, the second-order transition found for the broader Ising strips is the analog of the critical transition in the 2D Ising model. Note that such convergence was not observed for the narrower strips [cf. Fig. 6].

In addition to the prominent second-order transition a number of higher-order transition signals can be identified. The γ curves in Figs. 8(a) and (d) already hint at two other significant transitions; one in the upper-critical and the other in the subcritical regime.

Employing our classification scheme, the lowest-order transition at energies above the critical energy (or, equivalently, temperature above the critical temperature) is of third order and its existence depends on the second-order transition described above. As Figs. 9(a) and (b) show, the transition point does not show any convergence toward the critical point and, like in the 2D Ising case [5, 8], we conclude that this is a separate transition in the paramagnetic phase. Since it is dependent on the second-

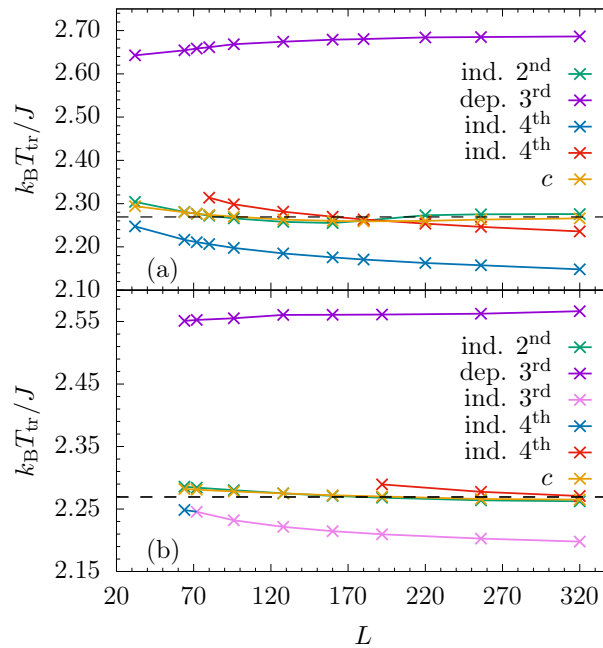


Figure 9. Microcanonical transition temperatures and peak temperatures of the specific heat curves c versus strip length L for (a) $M = 32$ and (b) $M = 64$ (lines are guides to the eye). The dashed lines mark the critical temperature of the 2D Ising model in the thermodynamic limit, $k_B T_c / J = 2 / \ln(1 + \sqrt{2})$.

order transition, one may want to interpret it a precursor of the latter. As the insets in the respective Figs. 8(b) and (e) of the third entropy derivative $\delta(e)$ show, the peak heights associated with this transition signal are very robust and do not change much upon increasing the strip length.

The other noteworthy transition develops in the subcritical regime. It is signaled by the lowest-energy peaks in Fig.8(c) near $e \approx -1.6$ for $M = 32$ and the developing local minimum in Fig. 8(e) at about $e \approx -1.55$ for $M = 64$. It is an independent transition of fourth order for all strip lengths studied and width $M = 32$, and turns into a third-order independent transition for $M = 64$ if $L \geq 72$. As can be seen in Figs. 9(a) and (b), this transition also seems to converge toward a transition point away from the critical point. This transition line was observed in the 2D Ising case as well [5, 8], see Fig. 2. In fact, as exemplary tests we performed show, strips with $M \geq 64$ behave very similar to the full 2D Ising system; the second-order transition (which becomes critical in the thermodynamic limit) and the two additional third-order transitions consolidate.

These two transitions seem to bracket what one might want to call the “critical atmosphere” around the critical point. There is an additional independent fourth-order transitions in the vicinity of the critical point which we included in Figs. 9(a) and (b). For $M = 32$ we clearly see it crossing the critical transition, which may indicate a qualitative change in the system that is unrelated to the ferromagnetic-paramagnetic transition.

Higher-than-fourth-order transitions were not included in our analysis, because the relevance of a transition signal diminishes with increasing order. Nonetheless, an in-depth discussion of the individual transition behavior and characteristics of Ising systems may require the consideration of additional precursor signals.

Finally, we would like to remark that the peaks observed in the specific heat curves for the broader Ising strips in Fig. 7 indeed indicate the onset of the critical transition. As the c line in Fig. 9 shows, the peak temperatures converge to the critical temperature known from the 2D Ising system. This was neither the case for the 1D system nor for the narrow strips with $M = 3$ and $M = 4$, which suggests that the qualitative cooperative behavior of spins in Ising strips changes between $M = 4$ and $M = 32$.

5. Conclusion

By means of exact statistical analysis, we identified and classified transition features in ferromagnetic one-dimensional Ising chains and two-dimensional Ising strips for various finite sizes. For this purpose, we employed the algorithmic approach proposed by Beale [6] for the exact evaluation of the number of states. The logarithm of this quantity can be interpreted as the microcanonical (energy-dependent) entropy. We then used the generalized microcanonical least-sensitive inflection-point analysis method [5] to systematically identify and classify transition signals in the entropy and its derivatives. We contrasted these results with features represented by extremal energetic fluctuations, i.e., maxima in corresponding (canonical) specific-heat curves, which are often used as indicators of transitions in systems of finite size (most prominently in thermodynamic studies of biological processes such as the folding of proteins, for which the thermodynamic limit is nonsensical due to the intrinsic disorder in their primary amino-acid sequence).

As expected, the microcanonical analysis of the one-dimensional Ising chain did not reveal any transition signals. Neither could we locate least-sensitive inflection points for finite chain lengths, nor did the extrapolation toward larger systems hint at potential transitions for the infinitely long chain. This is consistent with the historic findings for this system. It is worth noting that the specific heat curves in fact *do exhibit a peak*, which converges to a finite value in the thermodynamic limit. However, this extremal energetic fluctuation cannot be associated with any transition feature, even for finite systems, as there is no support for it by microcanonical analysis. Thus, we conclude that considering only extremal fluctuations in canonical response quantities as indicators for transitions may be misleading in the analysis of qualitative macroscopic changes in finite systems upon changing external state variables such as the canonical (heat-bath) temperature.

We then turned our attention to effectively two-dimensional Ising strips. For different constant strip widths $M = 3, 4, 32, 64$ we systematically extended the strip lengths L to find trends for transition signals. Like in the 1D case, we exclusively used the exact Beale solutions for the density of states to avoid numerical errors (the use of

Monte Carlo simulations and finite-size scaling analysis to consolidate our results is a future project). In all cases studied, the maxima of the specific heat curves do not show any trend to grow beyond finite limiting values. In fact, the narrower strips ($M = 3, 4$) behave like a one-dimensional Ising chain. For the broader strips ($M = 32, 64$), the peak region is significantly narrower, suggesting a qualitative change in the crossover regime between paramagnetic and ferromagnetic states. As expected, the specific-heat curves are not very helpful in revealing more specific information.

However, microcanonical inflection-point analysis enables a more diverse discussion. For all strip widths, and in contrast to the 1D case, we find a second-order transition, which we expect to be the analog of the critical transition in the full 2D case. For the narrower strips, the transition temperature does not show any tendency to converge toward the critical temperature, but settles at a larger value. Remarkably, the results for the broader Ising strips suggest that the observed second-order transition is closely related to the critical transition, despite the finite widths of the strips. In these cases, the second-order transition temperatures do converge to the critical value as the strip length is increased. For the broader strips, the microcanonically determined second-order transition temperatures correspond very well to the peak locations of the specific heat curves.

Like for the 2D Ising model on the square lattice [5, 8], we identify a number of additional transitions of higher order. Most striking are the dependent third-order transitions in the paramagnetic phase for $M = 32, 64$, which do not show indications of disappearing in the thermodynamic limit, although they do not seem to be linked to any catastrophic singularity in the thermodynamic limit either, which is probably the reason why to the best of our knowledge these signals have not been reported until recently [5, 8]. Since this transition is inevitably linked to the second-order transition, we consider it a precursor of the latter in the paramagnetic phase.

The lowest-temperature transitions we find occur in the ferromagnetic phase of the $M = 32$ and $M = 64$ systems and are independent of the critical transition. There is no tendency of the transition line to merge with the critical (or second-order) transition in the thermodynamic limit either. For $M = 32$ this transition is of fourth order, but rises to third order for sufficiently long $M = 64$ strips. This transition does also exist for the Ising system on the square lattice [5, 8].

The investigation of these transitions for larger systems requires Monte Carlo simulations and is left to future work. This will also allow the characterization of the additional (non-critical) transitions by systematically analyzing structural properties of spin configurations.

Acknowledgments

We would like to thank Kevin Bassler for helpful discussions.

References

- [1] Lenz W 1920 Beitrag zum Verständnis der magnetischen Erscheinungen in festen Körpern *Z. Phys.* **21** 613
- [2] Ising E 1925 Beitrag zur Theorie des Ferromagnetismus *Z. Phys.* **31** 253
- [3] Onsager L 1944 Crystal Statistics. I. A Two-Dimensional Model with an Order-Disorder Transition *Phys. Rev.* **65** 117
- [4] Bachmann M 2014 *Thermodynamics and Statistical Mechanics of Macromolecular Systems* (Cambridge: Cambridge University Press)
- [5] Qi K and Bachmann M 2018 Classification of Phase Transitions by Microcanonical Inflection-Point Analysis *Phys. Rev. Lett.* **120** 180601
- [6] Beale P D 1996 Exact Distribution of Energies in the Two-Dimensional Ising Model *Phys. Rev. Lett.* **76** 78
- [7] Kaufman B 1949 Crystal Statistics. II. Partition Function Evaluated by Spinor Analysis *Phys. Rev.* **76** 1232
- [8] Sitarachu K and Bachmann M 2019 Phase Transitions in the Two-Dimensional Ising Model from the Microcanonical Perspective, *J. Phys. Conf. Ser.* **1483** 012009
- [9] Landau D P and Binder K 2009 *A Guide to Monte Carlo Simulations in Statistical Physics* (Cambridge: Cambridge University Press)
- [10] Beekman A J, Rademaker L, and van Wezel J 2019 An Introduction to Spontaneous Symmetry Breaking, *SciPost Phys. Lect. Notes* **11**
- [11] Gross D H E 2001 *Microcanonical Thermodynamics* (Singapore: World Scientific)
- [12] Schnabel S, Seaton D T, Landau D P, and Bachmann M 2011 Microcanonical Entropy Inflection Points: Key to Systematic Understanding of Transitions in Finite Systems *Phys. Rev. E* **84** 011127
- [13] Stevenson P M 1981 Optimized Perturbation Theory *Phys. Rev. D* **23** 2916
- [14] Stevenson P M 1981 Resolution of the Renormalisation-Scheme Ambiguity in Perturbative QCD *Phys. Lett. B* **100** 61
- [15] Ehrenfest P 1933 Phasenumwandlungen im ueblichen und erweiterten Sinn, classifiziert nach den entsprechenden Singularitaeten des thermodynamischen Potentials *Proc. Royal Acad. Amsterdam (Netherlands)* **36** 153; *Commun. Kamerlingh Onnes Inst. Leiden* Suppl. No. 75b